

SPATIAL FEATURES OF ELECTOJETS DEVELOPMENT DURING NON-STORM SUPERSUBSTORMS: CASE STUDY

Irina Despirak¹, Natalia Kleimenova², Lyudmila Gromova³, Andris Lubchich¹

¹Polar Geophysical Institute, Apatity, Russia

²Schmidt Institute of Physics of the Earth, RAS, Moscow, Russia

³IZMIRAN, RAS, Troitsk, Moscow, Russia

e-mail: despirak@gmail.com

Keywords: Storm, Supersubstorm, Westward and eastward electrojets, Field-aligned currents (FAC)

Abstract: In our work we analyzed the magnetic disturbances and the global maps of field-aligned currents (FAC) during very intense substorm (SML<-2100 nT) on 22 April 2017 by the data from the global magnetometer networks SuperMAG, INTERMAGNET, IMAGE and data of from AMPERE projects. This event was selected because it was observed during non-storm conditions (SYM/H~-40 nT), while before that, all the considered events of supesubstorms (SSS) were observed against the background of the development of moderate or strong magnetic storms caused by coronal mass ejections (CME). We compare the spatio-temporal development of the electrojets during the storm and non-storm SSS events. It was shown that some specific features of the electrojets development, which were found for the storm SSS events, coincided with the behavior of the non-storm event of SSS. Namely, the global development of the westward electrojet was recorded from the dusk side (Alaska stations) to the dayside that, (IMAGE stations) of the Earth. Besides that, the strong eastward electrojet developed in the evening sector, which may be a result of the formation of an additional substorm current wedge (SCW) in the evening side. At the same time, the formation of this SCW and the occurrence of an additional upward field-aligned current were observed more strongly that during the storm-associated SSS events.

Introduction

The term “supersubstorms” was first introduced by investigations of very intense magnetic substorms from -the data of the SuperMag magnetometers network, the events with high negative values of SML index (< - 2500 nT) were called “supersubstorms” [1]. The SML index is calculated across the network of the SuperMAG stations [2].

The first studies indicated that SSSs have some features both in the space weather conditions during the appearance of SSSs and in the development of ground-based geomagnetic disturbances at this time. According to the papers [3, 4, 5], the SSSs are observed only under certain conditions in the solar wind: namely, the passage of magnetic clouds (MCs) or regions of compressed plasma in front of magnetic clouds (SHEATH), when there are jumps in the solar-wind pressure and large negative values of the Bz components of the Interplanetary Magnetic Field (IMF). In general, these conditions are also characteristic of the development of large magnetic storms. However, SSS events are not always associated with intense magnetic storms, as it would be logical to assume; they can also be observed during moderate magnetic storms and sometimes under non-storm conditions [1, 3]. The electrojets development during the SSSs, registered under the storm conditions, has been considered in some works, e.g., [4, 6, 7]. It was shown that the westward electrojet developed on a global scale by the longitude from the midnight to the afternoon sector surrounding the Earth. The highest intensity of the electrojet was observed at the auroral latitudes in the post-midnight time [4]. It is also shown that the strong eastward current was observed from after-noon to evening sector. The occurrence of an intense eastward electrojet supports the hypothesis of the formation of the additional ring current in the evening sector during the SSS [8].

We selected the events of the supersubstorms observed during the non-storm conditions, i.e. under the SYM/H- index > -50 nT. Only six such SSS events have been found in the 2010–2020 period, when the AMPERE observations were available. The SSS event of 22 April 2017 is studied in detail in this paper.

Data

The solar wind and IMF parameters are taken from the CDAWeb database and the catalog of large-scale solar wind types <ftp://ftp.iki.rssi.ru/pub/omni/catalog> [9]. Supersubstorm onset and

development were determined using the IMAGE and SuperMAG magnetometer data (<http://space.fmi.fi/image/>; <http://supermag.jhuapl.edu/>), besides some geomagnetic indexes SML, SMR and SMR_LT were used. SMR index calculation (as SYM/H index) is based on data of the N component with the baseline removed at available (~100 stations) ground magnetometer stations at geomagnetic latitudes between -50 and +50 degrees. Four local time sectors are defined with centers at 00, 06, 12, 18 MLT; the SMR value is $(SMR-00 + SMR-06 + SMR-12 + SMR-18)/4$ [10]. The global spatial distribution of electrojets was determined from the maps of magnetic field vectors obtained on the SuperMAG network, maps of spherical harmonic analysis of the distribution of magnetic vectors in the ionosphere and field-aligned currents obtained from the data of the low-apogee communication satellites Iridium of the AMPERE system (Active Magnetosphere and Planetary Electrodynamics Response Experiment, <http://ampere.jhuapl.edu>).

1. Interplanetary and geomagnetic conditions

Solar wind and interplanetary magnetic field (IMF) conditions for period of 21-26 April 2017 are shown in the Fig. 1a, from top to bottom: IMF magnitude (B_T), the IMF Y- and Z- components (B_Y , B_Z), the flow velocity (V), the dynamic pressure (P) and some geomagnetic indexes SYM/H and SML. It is seen that the features of the recurrent high-speed stream from coronal holes are observed in this period. At the front of the HSS, the region of the compressed plasma – the CIR- was registered. CIR and HSS boundaries are marked by the green and blue rectangles, respectively. The CIR contains the intervals of the negative values of the IMF B_z , but a magnetic storm was not developed (SYM/H ~ -40 nT). Against the background of CIR, at ~09:30 UT, one intense substorm (SML ~ -2100 nT) began to develop. The moment of the substorm onset is shown by the vertical red line. To describe the global development of a magnetic supersubstorm, we used the geomagnetic symmetric ring current index (SMR), divided by the MLT sectors (SMR_LT), which is shown in Fig. 1b. Different MLT sectors are shown with different colors on the SMR_LT plots: SMR_00 (blue), SMR_06 (green); SMR_12 (orange); SMR_18 (red). The index SML is shown for comparison. It is seen that the SMR_18, and SMR_12 ring-current intensities steadily increases and reach values ~ -80 nT at ~08 UT, before substorm. Then the SMR_18 plot shows the minimum at around ~09:30 UT, it corresponds to the SSS development. This proves that the ring current increased in the evening region of the magnetosphere during the SSS development.

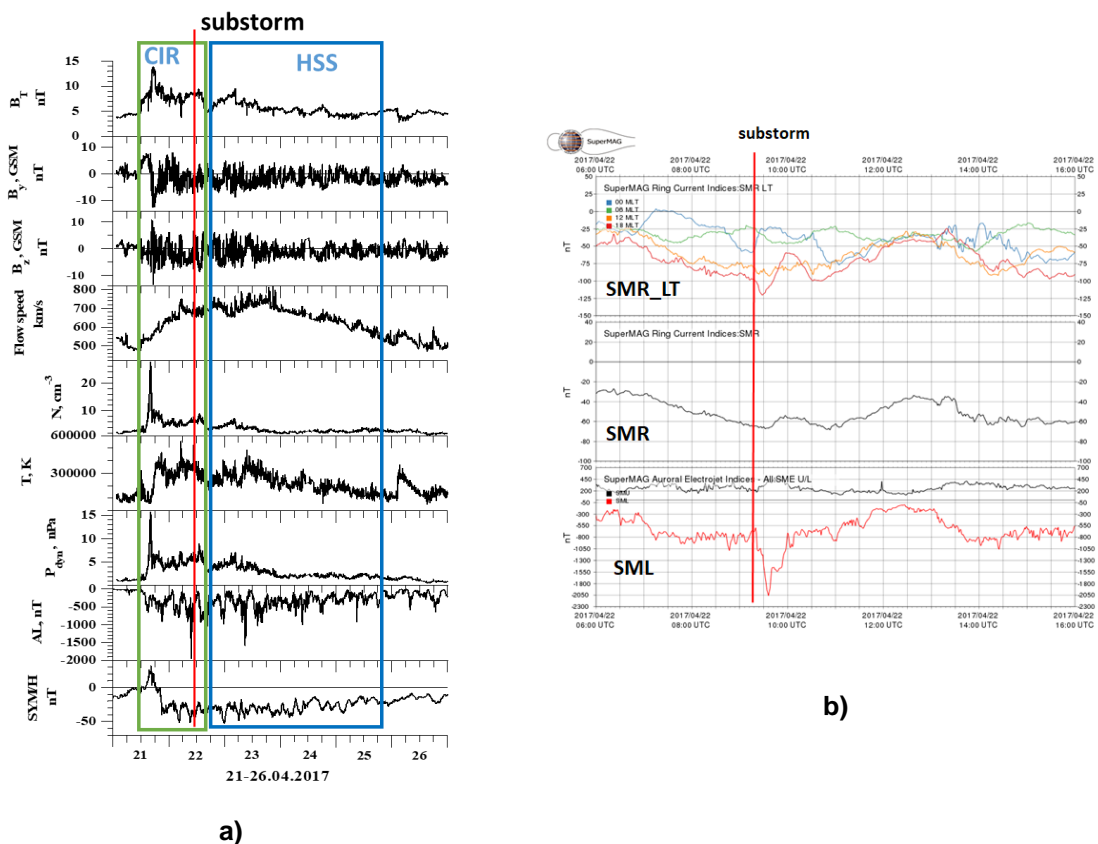


Fig. 1. a): Solar wind and IMF parameters on 21-26 April 2017. The CIR and HSS boundaries are marked by the green and blue rectangles, respectively; b): SMR-, SMR_LT and SML- indexes from 06 to 16 UT on 22 April 2017. The SSS onset is shown by the vertical red lines.

2. Magnetic observations

Ground-based magnetic disturbances during SSS are shown in Fig. 2. At the top panel, there is shown the global maps of the magnetic field vectors from the SuperMag data for 3 time moments, from the onset to maximal statement of the SSS development (Fig. 2a). It is seen that very strong disturbances were registered at Alaska stations (~ -2000 nT), the intense negative magnetic bays start at $\sim 09:15$ UT at DAW (66.2° MLAT; -85.3° MLON), CMO (65.4° MLAT; -93.8° MLON), BRW (70.6° MLAT; -106.5° MLON) and SIT (59.9° MLAT; -77.8° MLON) stations; the intensity of the negative bays was ~ -1300 - 2100 nT (Fig. 2c). Fig. 2b demonstrated that the negative bays in the X-component were registered at the BJN-NAL stations of the IMAGE network at ~ 9 - 10 UT, at the day sector (b). It is seen, that simultaneously with very intense disturbances in the night sector at Alaska stations, there were observed the bay-like magnetic disturbances located at the polar latitudes, at the stations BIN-NAL (near noon) (Fig. 2b and c).

Thus, during the SSS, the westward electrojet developed in the global scale (from before midnight, through the night and morning, into the day sector).

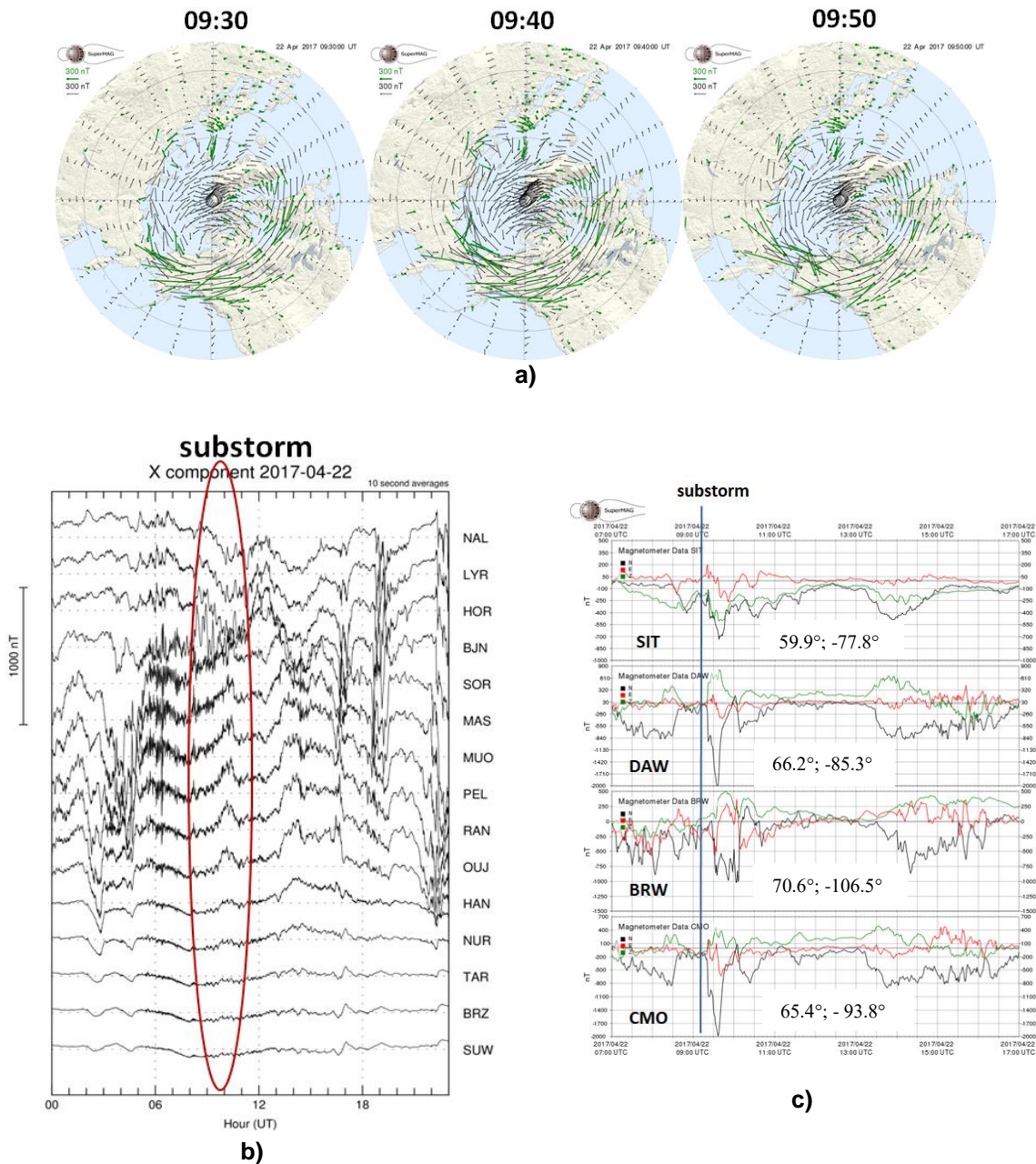


Fig. 2. Global maps of spatial distribution of the magnetic field vectors from the SuperMAG network during the onset and maximal phase of the SSS (a); X-component of magnetic field on SUW-NAL meridional chain of the IMAGE network on 22 April 2017 (b); N- (black line), E- (red line), Z- (green line) components of some stations of SuperMAG from 07 to 17 UT on 22 April 2017 (c)

3. Field-aligned currents from AMPERE observations

The AMPERE project represents the results of the magnetic registrations by the 66 satellites at 700 km altitude. In the Fig. 3, it is shown two maps of the spherical harmonic analysis of the magnetic registrations (the left panel) and calculated Field Aligned Currents (FAC) distribution (the right panel). The maps of the time of the SSS onset (~ 09:25 UT) and SSS maximal phase (~ 09:28 UT) are presented on the top and bottom panels. The upward Field Aligned Currents mark by red, the downward ones – by blue. Note, that the westward electrojet was located between the upward (red) and downward (blue) FAC; the eastward electrojet was located between downward (blue) and upward (red) currents.

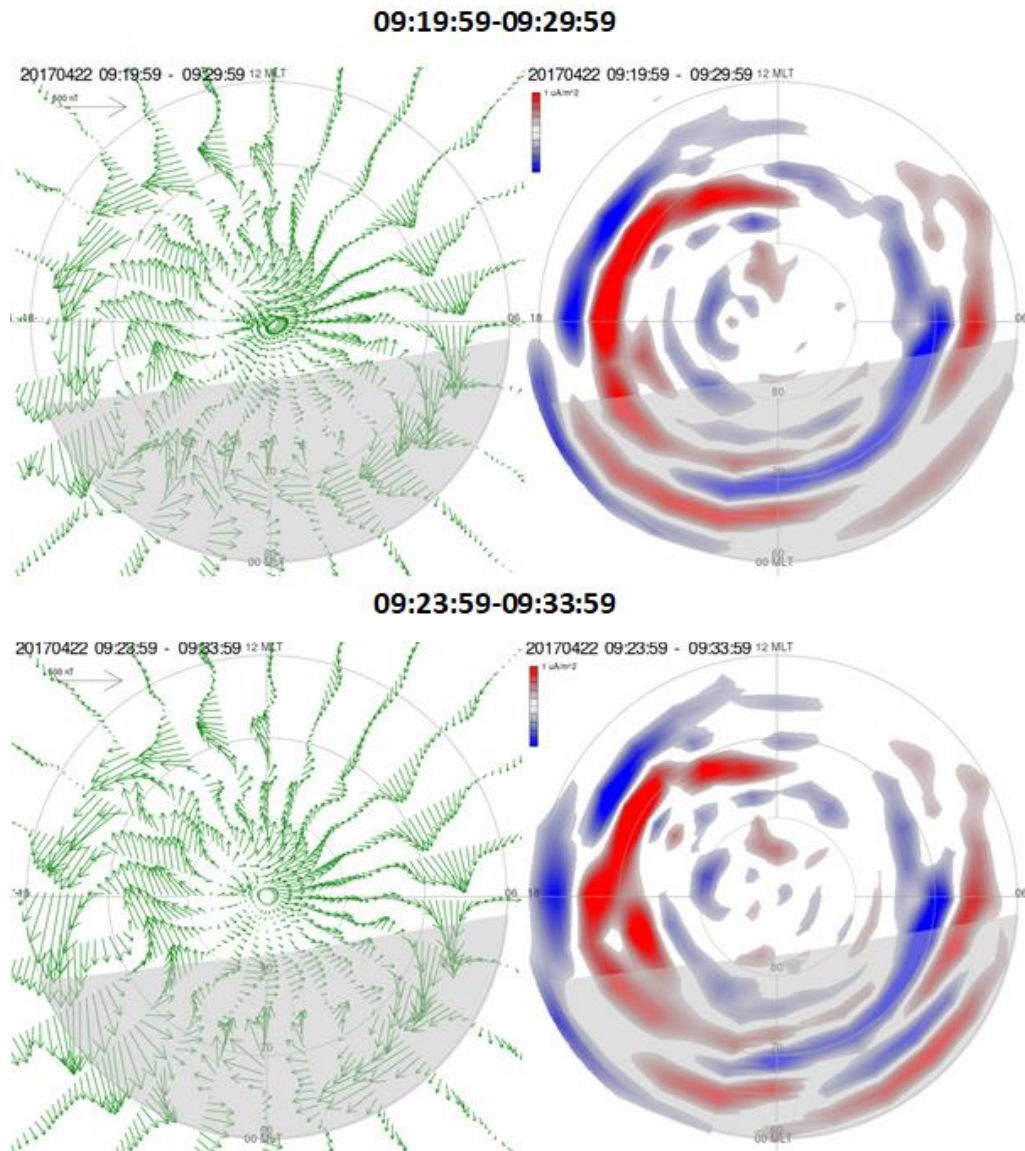


Fig. 3. Maps of the spherical harmonic analysis of the magnetic disturbance vectors and the Field Aligned Current distribution, calculated from the magnetic registrations according of the AMPERE data for two moments: at ~ 09:25 UT (top panels) and at ~ 09:28 UT (bottom panels) on April 22, 2017

The AMPERE maps demonstrate the global longitude expansion of the westward electrojet - from the pre-midnight sector of the auroral latitudes to the dayside of the polar area through the morning sector. In the evening sector (~18 MLT), there was observed the occurrence of an additional upward (red color) current, its growth and development is clearly seen in the bottom panel of Figure 3. Thus, the AMPERE maps also demonstrate the very strong enhancement of the eastward electrojet in the afternoon-evening sector. Note, that this fact supports the hypothesis of the formation of the additional ring current in the evening sector during SSS [8]. Zong et al. 2021 proposed, that the substorm current wedge (SCW) of supersubstorms significantly differs from the classical pattern of a SCW development.

We may estimate the development of the ring current using the SMR and SMR_LT-indexes calculated by SuperMAG data. The plots of the variations of the SMR- and SMR_LT- indexes on 22 April 2017 presented in Fig.1b. The moment of the SSS onset is shown by the vertical red line. It is seen that the SMR_18, and SMR_12 ring-current intensities steadily increases and reach values ~ 80 nT at ~ 08 UT, before the supersubstorm. The SMR_18 plot shows the minimum at around $\sim 09:30$ UT, which corresponds to the SSS development. This proves the ring current increasing in the evening region of the magnetosphere during the SSS development. Note, that, probably, this phenomenon is characteristic of the supersubstorms; this was also shown in [6], [7], [11]. However, in the considered event, observed during non-storm conditions, the occurrence of an additional upward FAC (Fig.3) and an additional ring current (Fig.1) were much stronger than during the storm-associated SSS events.

Summary

The comparison the behavior of the storm-associated and non-storm SSSs showed that some specific features of electrojets development are typical for both types of SSS events, namely:

- 1) The global development of westward electrojet from the dusk side (Alaska stations) to the day side (IMAGE stations);
- 2) The strong eastward electrojet development in the evening sector, probably, connected with the formation of an additional substorm current wedge in the evening side;
- 3) The occurrence of an additional upward Field Aligned Current in the evening sector.

Acknowledgements. The authors are grateful to the creators of the databases SuperMAG (SuperMAG: Products (jhuapl.edu)), IMAGE (<http://space.fmi.fi/image/>), AMPERE (<http://supermag.jhuapl.edu/>) for the opportunity to use them in this work. This study was supported by the RFBR (project number 20-55-18003) and National Science Fund of Bulgaria (NSFB) (project number КП-06-Русия/15).

References:

1. Tsurutani, B.T., R. Hajra, E. Echer, J.W. Gjerloev, Extremely intense ($SML \leq -2500$ nT) substorms: isolated events that are externally triggered? *Ann. Geophys.* 33, 519–524, 2015.
2. Gjerloev, J.W. The SuperMAG data processing technique, *J. Geophys. Res.*, 117(A9), A09213, 2012, <https://doi.org/10.1029/2012JA017683>
3. Despirak, I.V., A.A. Lyubchich, N.G. Kleimenova, Supersubstorms and conditions in the solar wind, *Geomag. Aeron.*, 59, no 2, 170–176, 2019.
4. Despirak, I.V., N.G. Kleimenova, L.I. Gromova, S.V. Gromov, L.M. Malysheva, Supersubstorms during storms of September 7–8, 2017, *Geomag. Aeron.*, 60, no 3, 308–317, 2020.
5. Hajra R., B.T. Tsurutani, E. Echer, W.D. Gonzalez, J.W. Gjerloev, Supersubstorms ($SML < -2500$ nT): Magnetic storm and solar cycle dependences, *J. Geophys. Res. Space Physics.* 121, 7805–7816, 2016, doi:10.1002/2015JA021835.
6. Despirak I.V., A.A. Lubchich, N.G. Kleimenova, L.I. Gromova, S.V. Gromov, L.M. Malysheva, Longitude geomagnetic effects of the supersubstorms during the magnetic storm of March 9, 2012. *Bulletin of the Russian Academy of Sciences: Physics*, 85, 3, 246–251, 2021.
7. Despirak I.V., N.G. Kleimenova, L.I. Gromova, A.A. Lubchich, V. Guineva, P.V. Setsko, Spatial features of supersubstorm in the main phase of the magnetic storm on 5 April 2010. *Bulletin of the Russian Academy of Sciences: Physics*, 86, 3, 249–255, 2022.
8. Zong, Q.-G., C. Yue, S.-Y. Fu, Shock induced strong substorms and super substorms: Preconditions and associated oxygen ion dynamics, *Space Sci. Rev.*, 217. <https://doi.org/10.1007/s11214-021-00806-x>, 2021.
9. Yermolaev, Yu.I., N.S. Nikolaeva, I.G. Lodkina, M.Yu. Yermolaev, Catalog of large-scale solar wind phenomena during 1976–2000, *Cosmic Res.*, 47, 2, 81–94, 2009.
10. Newell P.T., J.W., Gjerloev Evaluation of SuperMAG auroral electrojet indices as indicators of substorms and auroral power, *J. Geophys. Res.: Space Phys.*, 116, A12, A12211, 2011.
11. Despirak, I.V., N.G. Kleimenova, A.A. Lyubchich, P.V. Setsko, L.I. Gromova, R. Werner, Global Development of the Supersubstorm of May 28, 2011, *Geomag. Aeron.*, 62, 3, 308-317, 2022.